A combination of genome reduction and promoter engineering can enhance surfactin production by Bacillus amyloliquefaciens LL3

Fang Zhang
Nankai University
Kaiyue Huo
Nankai University
Xingyi Song
Nankai University
Yufen Quan
Nankai University
Weixia Gao
Tianjin University of Science and Technology
Shufang Wang
Nankai University
Chao Yang (yangc20119@nankai.edu.cn)
Nankai University https://orcid.org/0000-0002-7607-6621

Research

Keywords: Bacillus amyloliquefaciens, Genome reduction, promoter engineering, surfactin production

Posted Date: July 14th, 2020

DOI: https://doi.org/10.21203/rs.3.rs-41198/v1

Version of Record: A version of this preprint was published on December 7th, 2020. See the published version at https://doi.org/10.1186/s12934-020-01485-z.

Abstract

Background: Genome reduction and metabolic engineering have emerged as intensive research hotspots for constructing the optimal functional chassis and various microbial cell factories. Surfactin, a lipopeptide-type biosurfactant with broad spectrum antibiotic activity, has wide application prospects in anticancer therapy, biocontrol and bioremediation. *Bacillus amyloliquefaciens* LL3, previously isolated by our lab, contains an intact *srfA* operon in the genome for surfactin biosynthesis.

Results: In this study, a genome-reduced strain GR167 lacking ~4.18% of the *B. amyloliquefaciens* LL3 genome was constructed by deleting some unnecessary genomic regions. Compared with the strain NK-1 (LL3 derivative, Δ*upp*ΔpMC1), GR167 harbored faster growth rate, higher transformation efficiency, increased intracellular reducing power level and higher heterologous protein productivity. Furthermore, the optimal chassis GR167 was engineered for enhanced surfactin production. Firstly, the iturin and fengycin biosynthetic gene clusters were deleted from GR167 to generate GR167ID. Subsequently, two strong promoters PR_{suc} and PR_{tpxi} from LL3 were obtained by RNA-seq and promoter strength characterization, and then they were individually substituted for the native *srfA* promoter in GR167ID to generate GR167IDS and GR167IDT. The best mutant GR167IDS showed a 678-fold improvement in the transcriptional level of the *srfA* operon relative to GR167ID, and it produced 311.35 mg/L surfactin, with a 10.4-fold increase relative to GR167.

Conclusions: The genome-reduced strain GR167 was advantageous over the parental strain in several industrially relevant physiological traits assessed and it was highlighted as an optimum chassis for enhanced surfactin production. In future studies, further reduction of the LL3 genome can be expected to create high-performance chassis for synthetic biology applications.

Introduction

With the development of systems and synthetic biology, numerous studies have focused on the design and construction of the optimal functional microbial chassis with reduced genomes and superior physiological characteristics [1, 2]. Moderate genome reduction can create synthetic biology chassis with optimized genomic sequences, efficient metabolic regulatory networks and superior cellular physiological characteristics [3–5]. So far, several model microorganisms, such as *Escherichia coli* [6], *Bacillus subtilis* [7, 8] and *Pseudomonas putida* [9], have been intensively researched for minimal genome construction due to their clear genetic background and efficient genome editing approaches.

Surfactin, which contains a ring-shaped heptapeptide and a β-hydroxy fatty acid chain with 13–16 carbons, is a cyclic lipopeptide (CLP) biosurfactant with broad-spectrum antibiotic activity and mainly produced by *Bacillus* sp. via multifunctional non-ribosome peptide synthases (NRPSs) encoded by the *srfA* operon containing four open reading frames (*srfAA*, *srfAB*, *srfAC* and *srfAD*) [10, 11]. Surfactin has wide application prospects in biocontrol, bioremediation, food preservation and anticancer therapy [10, 12].

In recent years, several metabolic engineering strategies have been proposed for enhancing biosurfactant production, mainly including promoter engineering [13–15], the reduction of by-product formation [16], the enhancement of the precursor supply [2], the improvement of biosurfactant transmembrane efflux [17], and the modification of global regulatory factors [15, 16]. Among which, promoter engineering is highlighted as a powerful tool for enhancing the titer of biosurfactants. For example, the titer of iturin A was increased from an undetectable level to 37.35 mg/L by inserting a strong promoter C2up into upstream of the *itu* operon in *B. amyloliquefaciens* [15]. In another study, the titer of surfactin in *B. subtilis* was elevated from 0.07 g/L to 0.26 g/L by the replacement of the native *srfA* promoter with a constitutive promoter P_{veg} [18]. In addition to the natural promoters, Jiao et al [14] developed a chimeric promoter Pg3 for driving the synthesis of surfactin, resulting in a 15.6-fold increase in the titer of surfactin relative to the wild-type *B. subtilis* THY-7. However, efficient promoters need to be explored for the enhancement of biosurfactants production by members of the genus *Bacillus*.

Currently, endogenous promoters are highlighted as promising candidates for improved production of bacterial secondary metabolites [19]. For example, 14 endogenous promoters identified from *Streptomyces albus* J1074 by RNA-seq and reporter assays were successfully used to activate a cryptic gene cluster in *S. griseus* [20]. In another study, four endogenous promoters identified from *S. coelicolor* M145 by RNA-seq and reporter assays were used to activate cryptic biosynthetic clusters for jadomycin B production in *S. venezuelae* ISP5230 [9].

B. amyloliquefaciens LL3 was isolated initially for poly-γ-glutamic acid (γ-PGA) production by our lab, and whole genome of LL3 is currently available in the GenBank database (accession no. NC_017190.1) [21]. LL3 has a genomic size of 3,995,227 bp with an average G + C content of 45.7% and a circular plasmid (pMC1) of 6,758 bp. In particular, an intact *srfA* operon was found in the genome of LL3, suggesting the capability for surfactin biosynthesis. The essential genes and genomic islands (GIs) in LL3 were also identified by the Essential Genes Database (http://tubic.tju.edu.cn/deg/) and GIs Analysis Software (http://tubic.tju.edu.cn/GC-Profile/). Previously, a marker-free large fragments deletion method was well established in LL3 [22]. Therefore, previous studies have laid a foundation for genome reduction and enhanced surfactin production in LL3.

In this study, a genome-reduced strain GR167 was constructed from *B. amyloliquefaciens* NK-1 (LL3 derivative, Δ*upp*ΔpMC1) [23] and evaluated as an optimum chassis for several physiological traits. Furthermore, GR167 was engineered using metabolic engineering strategies for enhanced surfactin production.

Results And Discussion

Construction of a genome-reduced *B. amyloliquefaciens* strain GR167

To adapt to the adverse environmental conditions, there is a common mechanism horizontal gene transfer (HGT) among microorganisms, enabling host bacteria to acquire larger DNA segments, i.e., GIs,

the G+C contents of which are significantly different from that of the core genome [24]. GIs usually carry some functional genes related to pathogenicity and antibiotic resistance, leading to the emergence of multiple resistant bacteria by HGT [25]. In addition, there are latent secondary metabolic biosynthesis gene clusters scattered across the LL3 genome, which may increase the metabolic burden on cells and the purification cost of target products [26]. Consequently, to streamline the genome of LL3, the GIs containing putative protein genes, antibiotic biosynthesis genes and prophage protein genes, where the G+C contents deviate significantly from 45.7%, were selected as the knockout targets. Besides, the gene clusters *eps*, *bae* and *pgsBCA* responsible for the biosynthesis of extracellular polysaccharides, bacillaene and γ-PGA, respectively, which consume more energy and substrates, were also deleted from the LL3 genome. The detailed information on the deleted regions is summarized in Table S1. The schematic diagram for deletion of large genomic segments in LL3 is presented in Figure S1. Overall, a genome-reduced strain GR167 lacking ~4.18% of the LL3 genome was generated from NK-1 via a markerless deletion method [22]. The exact coordinates (G1 to G6) of the deleted regions on chromosome and the physical map of the endogenous plasmid pMC1 are shown in Fig. 1a and b, respectively.

Deleting redundant genes from a bacterial genome is expected to create superior chassis cells for the industrial production of valuable bio-based chemicals. Due to the existence of unannotated genes in the LL3 genome and lack of insight into the interactions among known genes, several industrially-relevant physiological traits were evaluated to determine whether GR167 is an ideal chassis for enhanced production of surfactin.

Genome reduction can improve the growth rate of LL3

To evaluate the effect of non-essential genomic sequences on cell growth, the growth profiles of GR167 and its parental strain NK-1 were detected by following the optical density (OD_{600}) of cells cultured in both poor (M9 medium) and rich (LB medium) conditions. As shown in Fig. 2a, obviously, whether incubated in LB or M9 medium, GR167 grew faster and yielded higher biomass with approximately 1.5 and 1.2-fold higher at the plateau phase than that of NK-1, respectively. To further quantify the growth parameters, the maximum specific growth rates (μ_{max}) of both strains were determined during exponential growth (Fig. 2b). The μ_{max} values of GR167 were 23.7% and 67% higher than that of NK-1 when cultured in LB and M9 medium, respectively. Due to the block of secondary metabolite biosynthesis pathways, more energy and substrates were used for basal metabolism and cell proliferation in GR167. When cultured in M9 medium, the μ_{max} of NK-1 was only 0.185 ± 0.004 h^{-1}, with a 30.7% decrease relative to that measured in LB, while GR167 showed a similar growth behavior in both media, suggesting that nutrition may be one of the main growth-limiting factors for NK-1 but not for GR167.

Deletion of non-essential genes may perturb cellular metabolism and thus impair cell growth [27, 28]. On the contrary, the genome-reduced strain GR167 acquired beneficial growth fitness, which was in agreement with previous studies [29, 30]. Overall, in this study, there was a positive correlation between cell growth and cumulative deletions, and deleting ~4.18% of the LL3 genome did not affect cellular

viability of GR167. Moreover, the growth rates of GR167 outcompeted the parental strain under the tested culture conditions, making it a promising chassis for further genetic engineering.

Genome reduction can broaden the range of carbon sources utilized by LL3

To further evaluate the changes in the metabolic potential of GR167 and NK-1, their ability to utilize various substrates was analyzed by a GEN III MicroPlate containing 23 carbon sources tested. As shown in Table 1, the substrates utilized by GR167 and NK-1 were significantly different with each other. Eight carbon sources could be efficiently metabolized by GR167, especially L-aspartate and methyl pyruvate, with a 30% and 43% increase in the utilization ratio compared to NK-1, respectively, suggesting that genome reduction may improve the capacity of LL3 to utilize certain substrates.

Genome reduction can improve transformation efficiency

An ideal chassis cell is expected to possess the excellent capacity to take up exogenous plasmids. As shown in Fig. 2c, when transformed with plasmid pHT01, GR167 surpassed the transformation efficiency of the parental strain NK-1 by about 137%. The GIs and BGCs deleted in this study may contain negative regulators related to transformation efficiency, making competent cells in the optimal DNA uptake state during electroporation. Li et al [4] found that the transformation efficiency of genome-reduced strains decreased with cumulative genomic deletions. In addition, similar to the results of the transformation efficiency, the growth rates of all mutants were inferior to the parental strain [4]. In this study, on the contrary, both the growth rate and transformation efficiency of GR167 were obviously higher than that of NK-1 (Figs. 2a and 2c). Similarly, in another study, an *E. coli* mutant MDS12 lacking 8.1% of the genome of the parental strain also displayed a positive correlation between the growth parameters and transformation efficiency [26]. We therefore speculate that higher transformation efficiency may be associated with the improved growth fitness of GR167, notwithstanding which may be a synergistic effect caused by many physiological characteristics [31].

Genome reduction can increase intracellular reducing power and the productivity of heterologous proteins

The intracellular reducing power ($NADPH/NADP^+$), which is indispensable for basic anabolic processes [32], was measured in this study. The intracellular $NADPH/NADP^+$ ratio of GR167 increased by 21.4% compared to the parental strain NK-1 (Fig. 2d), which may be attributed to the deletion of some NADPH-consuming biosynthesis pathways such as γ-PGA biosynthesis [33]. The improvement of intracellular reducing power level may be beneficial for GR167 to act as an ideal chassis for enhanced production of secondary metabolites.

Also, an optimal chassis is expected to possess high heterologous protein productivity. In a previous study, prophage and hypothetical proteins accounting for 45.6% and 54.4% of the genome of *Lactococcus lactis* NZ9000, respectively, were deleted, resulting in a significant increase in the production capability of red fluorescent protein [5]. In another study, a genome-reduced strain EM383 was

constructed from *P. putida* KT2440 by deleting flagellar operon and prophage protein genes, leading to a 40% increase in the production capability of foreign proteins [34].

In this study, GFP was selected as a model protein to determine the heterologous protein productivity. As shown in Fig. 2e, when transformed with plasmid pHT-P_{43}-*gfp*, the relative fluorescence intensity of GR167 was 50.4% higher than that of NK-1, indicating that the productivity of heterologous proteins was significantly improved by genome reduction.

Use of genome-reduced strain GR167 as an optimal chassis for surfactin production

For surafctin, it can hardly achieve a significant breakthrough in production only through traditional fermentation optimization because of its low yield in wild strains [14, 35]. Strategies for surfactin overproduction were focused on strain modification recent years, such as substitution of the native promoter P_{srf} of *srfA* operon [13, 14], overexpressing transporters to enhance surfactin efflux [17], and modifying the regulators ComX and PhrC [35]. However, most modifications were performed in existing strains. In our study, a genome-reduced strain GR167 with intact surfactin synthase operon was evaluated as an ideal chassis for its superior physiological characteristics. Engineering and modifying microbial chassis may maximize its practical application ranges and obtain maximum theoretical yields of bioproducts of interests. In a previous study, by deleting and co-overexpressing specific genes conducive to guanosine accumulation in a genome-reduced strain *B. subtilis* BSK814, the guanosine titer in the final strain was 4.4-fold higher than that in the control strain bearing the same genetic modifications [4]. In another study, BSK814 was also endowed with the ability to produce acetoin using xylose as carbon source by modifying xylose utilization related pathways [36]. Therefore, genome reduction may provide a desirable chassis for further strain modification, and metabolic engineering of genome-reduced strains may be more beneficial to the development of microbial cell factories.

As shown in Fig. 3, surfactin production by GR167 was demonstrated by high-performance liquid chromatography (HPLC). Compared with NK-ΔLP (NK-1 derivative, Δ*pgsBCA*) [37], a slight increase in the surfaction titer was observed with GR167. Consequently, it is interesting and necessary to explore whether microbial cell factories with high surfactin production capabilities can be constructed by further modification of GR167.

Enhancing surfactin production by blocking the potential competitive pathways

A transcriptional comparison between *B. amyloliquefaciens* LL3 and NK-ΔLP using RNA-seq revealed that the transcriptional levels of the gene clusters *srfA*, *itu* and *fen*, responsible for surfactin, iturin A and fengycin biosynthesis were all up-regulated (unpublished data). Iturin A and fengycin belonging to CLP antibiotics are structural analogues of surfactin [38], possibly leading to the reduction of the purity of the extracted surfactin from the culture supernatant. Iturin A and fengycin are synthesized by NRPSs like surfactin [11]; thus, they may share similar biosynthesis mechanisms with surfactin and their biosynthesis may compete for NADPH, energy and direct precursors with surfactin biosynthesis. In this study, the gene clusters *itu* (37.2 kb) and *fen* (11.5 kb) were deleted to enhance surfactin production. The

resulting mutants were designated as GR167I (Δ*itu*), GR167D (Δ*fen*) and GR167ID (Δ*itu*, Δ*fen*). The titer of surfactin was increased to 32.88 mg/L in GR167ID, with a 10% and 56% improvement in the titer and specific productivity of surfactin compared to GR167, respectively (Fig. 4). We speculate that blocking the potential competitive pathways may eliminate the competition for the same amino acid precursors, allowing for the redistribution of substrates towards surfactin biosynthesis.

Construction of endogenous promoter library of *B. amyloliquefaciens* LL3

Promoter engineering is considered as a promising approach for enhanced production of bacterial secondary metabolites [9, 19, 20]. FPKM (fragements per kilobase million) value is positively correlated with the transcriptional activity of a gene [39], which therefore can be regarded as an indicator for initial screening of promoters. Through RNA-seq analysis of LL3, all genes were ranked and classified into three groups based on their FPKM values, i.e., lower than 1,250, 1,250-4,000 and higher than 4,000. Then, the first six genes with higher FPKM values in each group were selected, and their upstream regions were predicted and cloned as described in Methods, named PR_x [*x*: the name of various related genes; PR: the sequences of predicted promoters with their ribosomal binding sites (RBSs)] and represented weak, moderate and strong promoters, respectively (Table 2). Subsequently, various reporter gene vectors derived from pHT01 containing fused fragments of the predicted promoters and *gfp* gene were used to assess the strengths of the tested promoters in LL3.

Characterization of the selected promoters via qPCR (quantitative real-time PCR) and GFP fluorescence measurement

As shown in Fig. 5a, the relative transcriptional levels of the candidate promoters measured with reporter gene vectors were PR_{ldh}, PR_{ahp}, PR_{hem}, PR_{tpxi}, PR_{clp}, PR_{suc}, PR_{accD}, PR_{gltA}, PR_{rpsu}, PR_{nfrA}, PR_{gltX}, PR_{ydh}, PR_{ugt}, PR_{arg}, PR_{nad}, PR_{lac}, PR_{alsD}, PR_{hom} and PR_{pgmi} in a descending order, which were inconsistent with the strengths of the promoters shown by the FPKM values (Table 2), with similar results reported in a previous study [19]. We speculate that the transcription of a gene on chromosome may be affected and regulated by flanking genes and regulatory sequences. However, this interference can be eliminated if a promoter is inserted into a plasmid.

To further determine the production capabilities of GFP, in this study, the relative fluorescence intensities of GFP were also measured in LL3. Among the 18 endogenous promoters, PR_{ahp} showed the strongest production capacity of GFP, followed by PR_{suc}, PR_{tpxi}, PR_{rpsU}, PR_{hem} and PR_{ydh} (Fig. 5b). However, the first six promoters were PR_{ldh}, PR_{ahp}, PR_{hem}, PR_{tpxi}, PR_{clp} and PR_{suc} from high to low at the transcriptional levels (Fig. 5a). Considering the different RBSs located upstream of the promoters evaluated in this study, we speculate that the different RBSs may affect the translational initiation efficiencies of mRNA corresponding to GFP, leading to the different trends between the transcriptional level and production capacity of GFP.

Substitution of the native *srfA* promoter enhanced surfactin production

Considering the heterologous expression of *srfA* is challenging for which large genetic sequence (over 25 kb) [40], substitution of the native *srfA* promoter by strong promoters is considered more beneficial for enhanced transcription of *srfA* operon [13, 14, 18]. For example, Sun et al [13] replaced the native P_{srf} promoter of *B. subtilis*, resulting in a 10-fold improvement in the titer of surfactin. In this study, two strong promoters PR_{suc} and PR_{tpxi}, of which nucleotide sequences are shown in supplementary material, derived from endogenous promoter library of LL3, were integrated into upstream of the *srfA* operon in GR167ID to construct surfactin hyperproducers GR167IDS and GR167IDT. As expected, both the surfactin production and specific productivity exhibited a significant elevation (Fig. 6a and b). In particular, the PR_{suc} promoter-substituted strain GR167IDS produced 311.35 mg/L surfactin, which was about 9.5-fold higher than that of GR167ID (Fig. 6a). Meanwhile, the transcriptional level of *srfA* operon in GR167IDS was 678-fold higher than that in GR167ID (Fig. 6c), indicating that the endogenous promoter PR_{suc} could significantly improve surfactin production by enhancing the transcription of *srfA* operon in *B. amyloliquefaciens* LL3.

Conclusions

In summary, a genome-reduced strain GR167 was constructed by deleting some non-essential genes accounting for ~ 4.18% of the LL3 genome and outcompeted the parental strain in several physiological traits assessed. GR167IDS, obtained from GR167 by promoter substitution, showed a 10.4-fold improvement in the titer of surfactin compared to GR167. The current results suggest that genome reduction in combination with promoter engineering may be a feasible strategy for the development of microbial cell factories capable of efficiently producing bacterial secondary metabolites.

Methods

Bacterial strains, media, and culture conditions

Escherichia coli DH5α was employed for plasmid construction and propagation. For the subsequent successful electroporation of *B. amyloliquefaciens* strains, the *E. coli* JM110 was used as intermediate host to demethylate the desirable plasmids from *E. coli* DH5α. *E. coli* strains were incubated at 37 °C in Luria–Bertani (LB) broth. *B. amyloliquefaciens* LL3 was deposited in the China Center for Type Culture Collection (CCTCC) (accession number: CCTCC M 208109). *B. amyloliquefaciens* NK-1 was employed as the parental strain for genome reduction. GR167 was used as the starting strain for engineered high-yielding surfactin producing mutants. All *B. amyloliquefaciens* strains were cultured in M9 mineral medium [41] and LB medium at 37 °C and 42 °C. For lipopeptide surfactin production, *B. amyloliquefaciens* was incubated at 30 °C and 180 rpm for 48 h in Landy medium [42]. When appropriate, media were supplemented with ampicillin (Ap; 100 μg/mL), chloramphenicol (Cm; 5 μg/mL) or 5-fluorouracil (5-FU; 1.3 mM).

Plasmid and strain construction

To construct the gene deletion vectors, the temperature-sensitive plasmid pKSU with an *upp* expression cassette was used [23]. The upstream and downstream fragments of the deleted genomic regions were amplified by PCR and then the two fragments were joined by overlap PCR. The generated fragment was ligated into pKSU via homologous recombination, to generate the gene deletion vectors. Introduction of plasmid into *B. amyloliquefaciens* was carried out using an optimized high osmolarity electroporation method [43]. To carry out multiple gene deletions on a single strain, a marker-less gene deletion method was used to construct the gene knockout mutants [22]. All the constructed plasmids and mutant strains were validated by PCR detection and DNA sequencing. All plasmids, strains, and primers used in this study are listed in Table 3, Table 4, and Table S2, respectively.

Physiological traits assessment

Growth profiles of GR167 and NK-1 were measured in both M9 mineral medium and LB medium. Overnight cultures (1 mL) were inoculated into 100 mL LB or M9 medium in 500-mL flasks and then incubated for 20 h at 37 °C and 180 rpm. To determine the bacterial growth status, the OD_{600} was monitored every 2 h using a UV-1800 spectrophotometer (Shimadzu, Kyoto, Japan).

The metabolic phenotypic analyses were performed with a Biolog GEN Ш MicroPlate™ using a phenotype microarray system (Biolog Inc., California, USA) according to the manufacturer's instructions. The bacterial cells on the solid medium surface were collected by cotton swab, dissolved into the inoculating fluid IF-B, and then the cell density was adjusted to a range of 80-86% Turbidity. Subsequently, 100 μl of bacterial suspensions were pipetted into the Biolog GEN Ш plates with different substrates. After the samples were incubated at 33 °C for 48 h, the absorbance at 590 nm was measured with the Biolog reader and the test data were analyzed by the Biolog system.

Electro-competent cells of GR167 and NK-1 (2×10^{10} CFU/mL) were prepared according to previous methods [15]. Subsequently, approximately 100 ng of plasmid pHT01 was absorbed by 100 μL of electro-competent cells via electroporation. After 3 h of incubation at 30 °C and 180 rpm, the mixture was spread on LB agar plates supplemented with 5 μg/mL Cm. The number of colonies was calculated to evaluate the transformation efficiency.

Cells were cultured in LB medium at 37 °C for 18 h. The intracellular cofactors NADPH and $NADP^+$ were extracted and quantified by enzymatic methods [44] using an EnzyChrom™ assay kit (BioAssay Systems, USA) according to the manufacturer's protocols.

The heterologous protein productivity was determined by introducing plasmid pHT-P_{43}-*gfp* into GR167 and NK-1. The detailed protocols for strain cultivation and fluorescence intensity measurement refer to our previous work [9]. The relative fluorescence intensity was normalized against per OD_{600} of whole cells. The fluorescence signal of NK-1 harboring pHT01 was set as background and was subtracted from overall fluorescence.

RNA-seq, promoter prediction, and construction of reporter gene vectors

RNA-seq analyses of LL3 were carried out according to our previous methods [33]. The expression levels of the predicted genes were quantified as the FPKM value [45]. The upstream regions of genes with different FPKM values were submitted online (http://www.fruitfly.org/seq_tools/promoter) for promoter prediction.

Furthermore, each promoter sequence plus its native RBS and *gfp* gene were amplified by PCR from the LL3 genome and pHT-P_{43}-*gfp*, respectively. Subsequently, 3'-end of a promoter sequence was fused with 5'-end of *gfp* gene and the fusion fragment was inserted into plasmid pHT01, to generate reporter gene vector pHT-PR_x-*gfp* for promoter strength characterization (Figure S2). Moreover, a control vector pHT-PR_{lac}-*gfp* with *gfp* expression driven by *lac* promoter was similarly constructed with pHT01.

Total RNA extraction, qPCR analyses, and GFP fluorescence measurement of reporter gene vectors

An appropriate number of cells from LB or Landy cultures were collected to isolate total RNA with the RNApure Bacteria kit (DNase I) (Cwbio, Beijing, China). Afterwards, complementary DNA (cDNA) was prepared with approximately 0.5 μg total RNA as template employing the HiScript® II Q RT SuperMix (Vazyme). To determine the transcriptional strength of relevant genes, qPCR analysis was carried out with ChamQ Universal SYBR qPCR Master Mix (Vazyme) and cDNA as the template. The relative gene transcription levels were calculated against that of *rpsU* gene as the internal standard [46]. The relative transcriptional activity of a promoter was normalized against that of *lac* promoter. In addition, GFP fluorescence measurement was performed as described previously [9].

Surfactin isolation and HPLC analyses

All tested strains were cultured aerobically at 180 rpm in the Landy medium for 48 h. The culture supernatant and bacterial cell were separated by centrifugation at 4 °C and 14,000 rpm for 20 min. Subsequently, the bacterial cell was lyophilized for 24 h and weighed. The supernatant was acidified to pH 2.0 with 6 M HCl and precipitated overnight at 4 °C. The precipitate formed was harvested by centrifugation and resuspended with 100 mL methyl alcohol. After which, 1 M NaOH was added to adjust the pH to 7.0 and further incubated for 48 h at 180 rpm and 37 °C. The supernatant containing surfactin extract was collected by centrifugation. Prior to HPLC analysis, the supernatant was filtered via a 0.22-μm filter and concentrated through a vacuum rotary evaporator. Surfactin was analyzed and quantified by HPLC equipped with a C18 column (Innoval ODS-2, 250 mm × 4.6 mm × 5 μm, Phenomenex, USA) using a validated method described previously [15, 45]. The extracted surfactin samples (20 μL) were injected into the HPLC system with a mobile phase consisting of acetonitrile and water (55:45, v/v) at a flow rate of 0.8 mL/min. Surfactin was detected at 210 nm.

Declarations

Funding

This work was supported by the National Key Research and Development Program of China (2018YFA0900100), the National Natural Science Funding of China (31670093) and the Tianjin Natural Science Funding (18JCYBJC24500).

Acknowledgements

All of the authors thank the editor and the anonymous reviewers for their valuable comments.

Authors' contributions

FZ and CY designed this study. FZ, YFQ and WXG performed these experiments. FZ, KYH, XYS, SFW carried out the data analysis. FZ and CY wrote the manuscript.

Availability of date and materials

All data generated or analyzed during the current study are included in this published article and its additional file.

Ethics approval and consent to participate

Not applicable.

Consent for publication

Not applicable.

Competing interests

The authors declare that they have no competing interests.

References

1. Koonin EV: Comparative genomics, minimal gene-sets and the last universal common ancestor. Nat Rev Microbiol. 2003;1:127-136. 2. Juhas M, Reuß DR, Zhu B, Commichau FM: Bacillus subtilis and Escherichia coli essential genes and minimal cell factories after one decade of genome engineering. Microbiology. 2014;160:2341-2351. 3. Leprince A, van Passel MW, dos Santos VA: Streamlining genomes: toward the generation of simplified and stabilized microbial systems. Curr Opin Biotechnol. 2012;23:651-658. 4. Li Y, Zhu X, Zhang X, Fu J, Wang Z, Chen T, Zhao X: Characterization of genome-reduced Bacillus subtilis strains and their application for the production of guanosine and thymidine. Microb Cell Fact. 2016;15:94. 5. Zhu D, Fu Y, Liu F, Xu H, Saris PE, Qiao M: Enhanced heterologous protein productivity by genome reduction in Lactococcus lactis NZ9000. Microb Cell Fact. 2017;16:1. 6. Mizoguchi H, Sawano Y, Kato J, Mori H: Superpositioning of deletions promotes growth of Escherichia coli with a reduced genome. DNA Res. 2008;15:277-284. 7. Morimoto T, Kadoya R, Endo K, Tohata M, Sawada K, Liu S, Ozawa T, Kodama T, Kakeshita H, Kageyama Y, et al: Enhanced recombinant protein productivity by

genome reduction in Bacillus subtilis. DNA Res. 2008;15:73-81. 8. Aguilar Suárez R, Stülke J, van Dijl JM: Less Is More: Toward a Genome-Reduced Bacillus Cell Factory for "Difficult Proteins". ACS Synth Biol. 2019;8:99-108. 9. Liang P, Zhang Y, Xu B, Zhao Y, Liu X, Gao W, Ma T, Yang C: Deletion of genomic islands in the Pseudomonas putida KT2440 genome can create an optimal chassis for synthetic biology applications. 2020, 19:70. 10. Deravel J, Lemière S, Coutte F, Krier F, Van Hese N, Béchet M, Sourdeau N, Höfte M, Leprêtre A, Jacques P: Mycosubtilin and surfactin are efficient, low ecotoxicity molecules for the biocontrol of lettuce downy mildew. Appl Microbiol Biotechnol. 2014;98:6255-6264. 11. Seydlová G, Svobodová JJCEJoM: Review of surfactin chemical properties and the potential biomedical applications. 2008;3:123-133. 12. Lai CC, Huang YC, Wei YH, Chang JS: Biosurfactant-enhanced removal of total petroleum hydrocarbons from contaminated soil. J Hazard Mater. 2009;167:609-614. 13. Sun H, Bie X, Lu F, Lu Y, Wu Y, Lu Z: Enhancement of surfactin production of Bacillus subtilis fmbR by replacement of the native promoter with the Pspac promoter. Can J Microbiol. 2009;55:1003-1006. 14. Jiao S, Li X, Yu H, Yang H, Li X, Shen Z: In situ enhancement of surfactin biosynthesis in Bacillus subtilis using novel artificial inducible promoters. Biotechnol Bioeng. 2017;114:832-842. 15. Dang Y, Zhao F, Liu X, Fan X, Huang R, Gao W, Wang S, Yang C: Enhanced production of antifungal lipopeptide iturin A by Bacillus amyloliquefaciens LL3 through metabolic engineering and culture conditions optimization. Microb Cell Fact. 2019;18:68. 16. Wu Q, Zhi Y, Xu Y: Systematically engineering the biosynthesis of a green biosurfactant surfactin by Bacillus subtilis 168. Metab Eng. 2019;52:87-97. 17. Li X, Yang H, Zhang D, Li X, Yu H, Shen Z: Overexpression of specific proton motive force-dependent transporters facilitate the export of surfactin in Bacillus subtilis. J Ind Microbiol Biotechnol. 2015;42:93-103. 18. Willenbacher J, Mohr T, Henkel M, Gebhard S, Mascher T, Syldatk C, Hausmann R: Substitution of the native srfA promoter by constitutive Pveg in two B. subtilis strains and evaluation of the effect on Surfactin production. J Biotechnol. 2016;224:14-17. 19. Zhao F, Liu X, Kong A, Zhao Y, Fan X, Ma T, Gao W, Wang S, Yang C: Screening of endogenous strong promoters for enhanced production of medium-chain-length polyhydroxyalkanoates in Pseudomonas mendocina NK-01. Sci Rep. 2019; 9:1798. 20. Luo Y, Zhang L, Barton KW, Zhao H: Systematic Identification of a Panel of Strong Constitutive Promoters from Streptomyces albus. ACS Synth Biol. 2015;4:1001-1010. 21. Geng W, Cao M, Song C, Xie H, Liu L, Yang C, Feng J, Zhang W, Jin Y, Du Y, Wang S: Complete genome sequence of Bacillus amyloliquefaciens LL3, which exhibits glutamic acid-independent production of poly-γ-glutamic acid. J Bacteriol. 2011;193:3393-3394. 22. Zhang W, Gao W, Feng J, Zhang C, He Y, Cao M, Li Q, Sun Y, Yang C, Song C, Wang S: A markerless gene replacement method for B. amyloliquefaciens LL3 and its use in genome reduction and improvement of poly-γ-glutamic acid production. Appl Microbiol Biotechnol. 2014;98:8963-8973. 23. Feng J, Gao W, Gu Y, Zhang W, Cao M, Song C, Zhang P, Sun M, Yang C, Wang S: Functions of poly-gamma-glutamic acid (γ-PGA) degradation genes in γ-PGA synthesis and cell morphology maintenance. Appl Microbiol Biotechnol. 2014;98:6397-6407. 24. Vernikos GS, Parkhill J: Resolving the structural features of genomic islands: a machine learning approach. Genome Res. 2008;18:331-342. 25. Jani M, Sengupta S, Hu K, Azad RK: Deciphering pathogenicity and antibiotic resistance islands in methicillin-resistant Staphylococcus aureus genomes. Open Biol. 2017;7. 26. Kolisnychenko V, Plunkett G, 3rd, Herring CD, Fehér T, Pósfai J, Blattner FR, Pósfai G: Engineering a reduced Escherichia coli genome. Genome Res. 2002;12:640-647. 27. Akeno Y, Ying BW, Tsuru S, Yomo T: A reduced genome decreases the host carrying

capacity for foreign DNA. Microb Cell Fact. 2014;13:49. 28. Unthan S, Baumgart M, Radek A, Herbst M, Siebert D, Brühl N, Bartsch A, Bott M, Wiechert W, Marin K, et al: Chassis organism from Corynebacterium glutamicum–a top-down approach to identify and delete irrelevant gene clusters. Biotechnol J. 2015;10:290-301. 29. Wenzel M, Altenbuchner J: Development of a markerless gene deletion system for Bacillus subtilis based on the mannose phosphoenolpyruvate-dependent phosphotransferase system. Microbiology. 2015;161:1942-1949. 30. Geissler M, Kühle I, Morabbi Heravi K, Altenbuchner J, Henkel M, Hausmann R: Evaluation of surfactin synthesis in a genome reduced Bacillus subtilis strain. AMB Express. 2019;9:84. 31. Hamoen LW, Venema G, Kuipers OP: Controlling competence in Bacillus subtilis: shared use of regulators. Microbiology. 2003;149:9-17. 32. Martínez I, Zhu J, Lin H, Bennett GN, San KY: Replacing Escherichia coli NAD-dependent glyceraldehyde 3-phosphate dehydrogenase (GAPDH) with a NADP-dependent enzyme from Clostridium acetobutylicum facilitates NADPH dependent pathways. Metab Eng. 2008;10:352-359. 33. Feng J, Quan Y, Gu Y, Liu F, Huang X, Shen H, Dang Y, Cao M, Gao W, Lu X, et al: Enhancing poly-γ-glutamic acid production in Bacillus amyloliquefaciens by introducing the glutamate synthesis features from Corynebacterium glutamicum. Microb Cell Fact. 2017;16:88. 34. Lieder S, Nikel PI, de Lorenzo V, Takors R: Genome reduction boosts heterologous gene expression in Pseudomonas putida. Microb Cell Fact. 2015; 14:23. 35. Jung J, Yu KO, Ramzi AB, Choe SH, Kim SW, Han SO: Improvement of surfactin production in Bacillus subtilis using synthetic wastewater by overexpression of specific extracellular signaling peptides, comX and phrC. Biotechnol Bioeng. 2012;109:2349-2356. 36. Yan P, Wu Y, Yang L, Wang Z, Chen T: Engineering genome-reduced Bacillus subtilis for acetoin production from xylose. Biotechnol Lett. 2018;40:393-398. 37. Feng J, Gu Y, Han L, Bi K, Quan Y, Yang C, Zhang W, Cao M, Wang S, Gao W, et al: Construction of a Bacillus amyloliquefaciens strain for high purity levan production. FEMS Microbiol Lett. 2015;362. 38. Zhao H, Shao D, Jiang C, Shi J, Li Q, Huang Q, Rajoka MSR, Yang H, Jin M: Biological activity of lipopeptides from Bacillus. Appl Microbiol Biotechnol. 2017;101:5951-5960. 39. Mortazavi A, Williams BA, McCue K, Schaeffer L, Wold B: Mapping and quantifying mammalian transcriptomes by RNA-Seq. Nat Methods. 2008;5:621-628. 40. Nakano MM, Magnuson R, Myers A, Curry J, Grossman AD, Zuber P: srfA is an operon required for surfactin production, competence development, and efficient sporulation in Bacillus subtilis. J Bacteriol. 1991;173:1770-1778. 41. Harwood CR, Cutting SM. Molecular biological methods for Bacillus. England: Wiley;1990. 42. Landy M, Rosenman SB, Warren GH: An antibiotic from Bacillus subtilis active against pathogenic fungi. J Bacteriol. 1947;54:24. 43. Zhang W, Xie H, He Y, Feng J, Gao W, Gu Y, Wang S, Song C: Chromosome integration of the Vitreoscilla hemoglobin gene (vgb) mediated by temperature-sensitive plasmid enhances γ-PGA production in Bacillus amyloliquefaciens. FEMS Microbiol Lett. 2013;343:127-134. 44. Bergmeyer HU, Bergmeyer J, Graßl M: Methods of enzymatic analysis. Verlag Chemie; 1984. 45. Gao W, Liu F, Zhang W, Quan Y, Dang Y, Feng J, Gu Y, Wang S, Song C, Yang C: Mutations in genes encoding antibiotic substances increase the synthesis of poly-γ-glutamic acid in Bacillus amyloliquefaciens LL3. Microbiologyopen. 2017;6. 46. Reiter L, Kolstø AB, Piehler AP: Reference genes for quantitative, reverse-transcription PCR in Bacillus cereus group strains throughout the bacterial life cycle. J Microbiol Methods. 2011;86:210-217.

Tables

Table 1 Profile of metabolic phenotype

Substrate utilization ratio compared with the parental strain NK-1 (%)					
Substrate	GR167	Substrate	GR167	Substrate	GR167
Methyl pyruvate	43	D-Sorbitol	-27	D- Mannose	-26
L-Aspartate	30	D-Maltose	-25	D- Fructose	-9
Tween 40	15	D-Trehalose	-33	Glycerol	-45
Methyl D-lactate	7	D-Cellobiose	-33	L-Glutamate	-5
Citric acid	5	Gentiobiose	-5	L-Lactic Acid	-3
L-Malic Acid	7	Sucrose	-20	γ-Amino-Butryric Acid	-20
Formic Acid	8	α-D- Lactose	-24	Acetoacetic Acid	-1
Acetic Acid	0.8	α-D- Glucose	-25		

Table 2 Endogenous promoters selected according to FPKM values

weak promoter		moderate promoter		strong promoter	
promoter[a]	FPKM[b]	promoter	FPKM	promoter	FPKM
PR_{ugt}	691	PR_{gltX}	1268	PR_{pgmi}	4143
PR_{suc}	701	PR_{nad}	1333	PR_{hom}	4737
PR_{ydh}	810	PR_{arg}	1480	PR_{hem}	7060
PR_{accD}	890	PR_{gltA}	1592	PR_{ldh}	7569
PR_{clp}	1024	PR_{ahp}	2079	PR_{rpsU}	16570
PR_{tpxi}	1243	PR_{nrfA}	2890	PR_{alsD}	28940

[a] The promoters were named according to relative genes, PR_{ugt} represents the original promoter and RBS (ribosome binding site) of *ugt* gene

[b] FPKM values from relative genes

Table 3 Plasmids used in this study

Plasmids	Relative characteristics	source
pKSU	pKSV7 derivative with *upp* gene, temperature-sensitive replication origin, Ap^r (gram-negative) and Cm^r (gram-positive)	[22]
pKSU-ΔG1	pKSU derivative, carrying deletion fragment of G1	This work
pKSU-ΔG2	pKSU derivative, carrying deletion fragment of G2	This work
pKSU-ΔG3	pKSU derivative, carrying deletion fragment of G3	This work
pKSU-ΔG4	pKSU derivative, carrying deletion fragment of G4	This work
pKSU-ΔG5	pKSU derivative, carrying deletion fragment of G5	This work
pKSU-ΔG6	pKSU derivative, carrying deletion fragment of G6	This work
pKSU-Δ*itu*	pKSU derivative, carrying deletion fragment of *itu*	This work
pKSU-Δ*fenD*	pKSU derivative, carrying deletion fragment of *fenD*	This work
pHT01	*E. coli-Bacillus* shuttle vector, Ap^r (gram-negative) and Cm^r (gram-positive)	This lab
pHT-P_{43}-*gfp*	pHT01 derivative, used for providing *gfp* gene	This lab
pBBR1MCS-2	expression plasmid used for providing *lac* promoter	This lab
pHT-PR_{lac}-*gfp*	pHT01 derivative, containing PR_{lac} promoter and *gfp* gene	This work
pHT-PR_{ugt}-*gfp*	pHT01 derivative, containing PR_{ugt} promoter and *gfp* gene	This work
pHT-PR_{suc}-*gfp*	pHT01 derivative, containing PR_{suc} promoter and *gfp* gene	This work
pHT-PR_{ydh}-*gfp*	pHT01 derivative, containing PR_{ydh} promoter and *gfp* gene	This work
pHT-PR_{accD}-*gfp*	pHT01 derivative, containing PR_{accD} promoter and *gfp* gene	This work
pHT-PR_{clp}-*gfp*	pHT01 derivative, containing PR_{clp} promoter and *gfp* gene	This work
pHT-PR_{tpxi}-*gfp*	pHT01 derivative, containing PR_{tpxi} promoter and *gfp* gene	This work
pHT-PR_{gltX}-*gfp*	pHT01 derivative, containing PR_{gltX} promoter and *gfp* gene	This work
pHT-PR_{nad}-*gfp*	pHT01 derivative, containing PR_{nad} promoter and *gfp* gene	This work
pHT-PR_{arg}-*gfp*	pHT01 derivative, containing PR_{arg} promoter and *gfp* gene	This work
pHT-PR_{gltA}-*gfp*	pHT01 derivative, containing PR_{gltA} promoter and *gfp* gene	This work
pHT-PR_{ahp}-*gfp*	pHT01 derivative, containing PR_{ahp} promoter and *gfp* gene	This work
pHT-PR_{nrfA}-*gfp*	pHT01 derivative, containing PR_{nrfA} promoter and *gfp* gene	This work
pHT-PR_{pgmi}-*gfp*	pHT01 derivative, containing PR_{pgmi} promoter and *gfp* gene	This work
pHT-PR_{hom}-*gfp*	pHT01 derivative, containing PR_{hom} promoter and *gfp* gene	This work
pHT-PR_{hem}-*gfp*	pHT01 derivative, containing PR_{hem} promoter and *gfp* gene	This work
pHT-PR_{ldh}-*gfp*	pHT01 derivative, containing PR_{ldh} promoter and *gfp* gene	This work
pHT-PR_{rpsU}-*gfp*	pHT01 derivative, containing PR_{rpsU} promoter and *gfp* gene	This work
pHT-PR_{alsD}-	pHT01 derivative, containing PR_{alsD} promoter and *gfp* gene	This work

gfp		
pKSU-PR$_{suc}$	pKSU derivative, containing PR$_{suc}$ flanked by upstream and downstream regions of *srf*	This work
pKSU-PR$_{tpxi}$	pKSU derivative, containing PR$_{tpxi}$ flanked by upstream and downstream regions of *srf*	This work

Cm^r, chloramphenicol resistance; Ap^r, ampicillin resistance

Table 4 Strains used in this study

Strains	Relative characteristics	source
B. amyloliquefaciens		
GR01	LL3 derivative, Δ*upp*	[22]
GR07 (NK-1)	GR01 ΔG0, 0.18% reduction of genome	[23]
GR22	GR07 ΔG1, 0.55% reduction of genome	This work
GR46	GR22 ΔG2, 1.15% reduction of genome	This work
GR94	GR46 ΔG3, 2.36% reduction of genome	This work
GR134	GR94 ΔG4, 3.36% reduction of genome	This work
GR164	GR134 ΔG5, 4.11% reduction of genome	This work
GR167	GR164 ΔG6, 4.18% reduction of genome	This work
NK-ΔLP	NK-1 derivative, Δ*pgsBCA*	[37]
GR167I	GR167 derivative, Δ*itu* cluster	This work
GR167D	GR167 derivative, Δ*fen* cluster	This work
GR167ID	GR167 derivative, Δ*itu* Δ*fen* clusters	This work
LL3-PR_{lac}	LL3 derivative, containing plasmid pHT-PR_{lac}-*gfp*	This work
LL3-PR_{ugt}	LL3 derivative, containing plasmid pHT-PR_{ugt}-*gfp*	This work
LL3-PR_{suc}	LL3 derivative, containing plasmid pHT-PR_{suc}-*gfp*	This work
LL3-PR_{ydh}	LL3 derivative, containing plasmid pHT-PR_{ydh}-*gfp*	This work
LL3-PR_{accD}	LL3 derivative, containing plasmid pHT-PR_{accD}-*gfp*	This work
LL3-PR_{clp}	LL3 derivative, containing plasmid pHT-PR_{clp}-*gfp*	This work
LL3-PR_{tpxi}	LL3 derivative, containing plasmid pHT-PR_{tpxi}-*gfp*	This work
LL3-PR_{gltX}	LL3 derivative, containing plasmid pHT-PR_{gltX}-*gfp*	This work
LL3-PR_{nad}	LL3 derivative, containing plasmid pHT-PR_{nad}-*gfp*	This work
LL3-PR_{arg}	LL3 derivative, containing plasmid pHT-PR_{arg}-*gfp*	This work
LL3-PR_{gltA}	LL3 derivative, containing plasmid pHT-PR_{gltA}-*gfp*	This work
LL3-PR_{ahp}	LL3 derivative, containing plasmid pHT-PR_{ahp}-*gfp*	This work
LL3-PR_{nrfA}	LL3 derivative, containing plasmid pHT-PR_{nrfA}-*gfp*	This work
LL3-PR_{pgmi}	LL3 derivative, containing plasmid pHT-PR_{pgmi}-*gfp*	This work
LL3-PR_{hom}	LL3 derivative, containing plasmid pHT-PR_{hom}-*gfp*	This work
LL3-PR_{hem}	LL3 derivative, containing plasmid pHT-PR_{hem}-*gfp*	This work
LL3-PR_{ldh}	LL3 derivative, containing plasmid pHT-PR_{ldh}-*gfp*	This work
LL3-PR_{rpsU}	LL3 derivative, containing plasmid pHT-PR_{rpsU}-*gfp*	This work
LL3-PR_{alsD}	LL3 derivative, containing plasmid pHT-PR_{alsD}-*gfp*	This work
GR167IDS	GR167ID derivative with its native *srf* promoter replaced by PR_{suc} promoter	This work
GR167IDT	GR167ID derivative with its native *srf* promoter replaced by PR_{tpxi} promoter	This work
E. coli strains		
DH5α	*supE44* Δ*lacU169*(_*80 lacZ*ΔM15) *recA1 endA1 hsdR17*(r_K^- m_K^+) *thi-1gyrA relA1* F^- Δ(*lacZYA-argF*)	Transgene
JM110	F^-*dam*-13::Tn9 (Cam^r) *dcm*-6 *hsdR2* ($r_k^-m_k^+$) *leuB6 hisG4 thi-1 araC14 lacY1 galK2 galT22 xylA5 mtl-1 rpsL136* (Str^r) *fhuA31 tsx-8 glnV*44 *mcrA mcrB*1	Fermentas

Figures

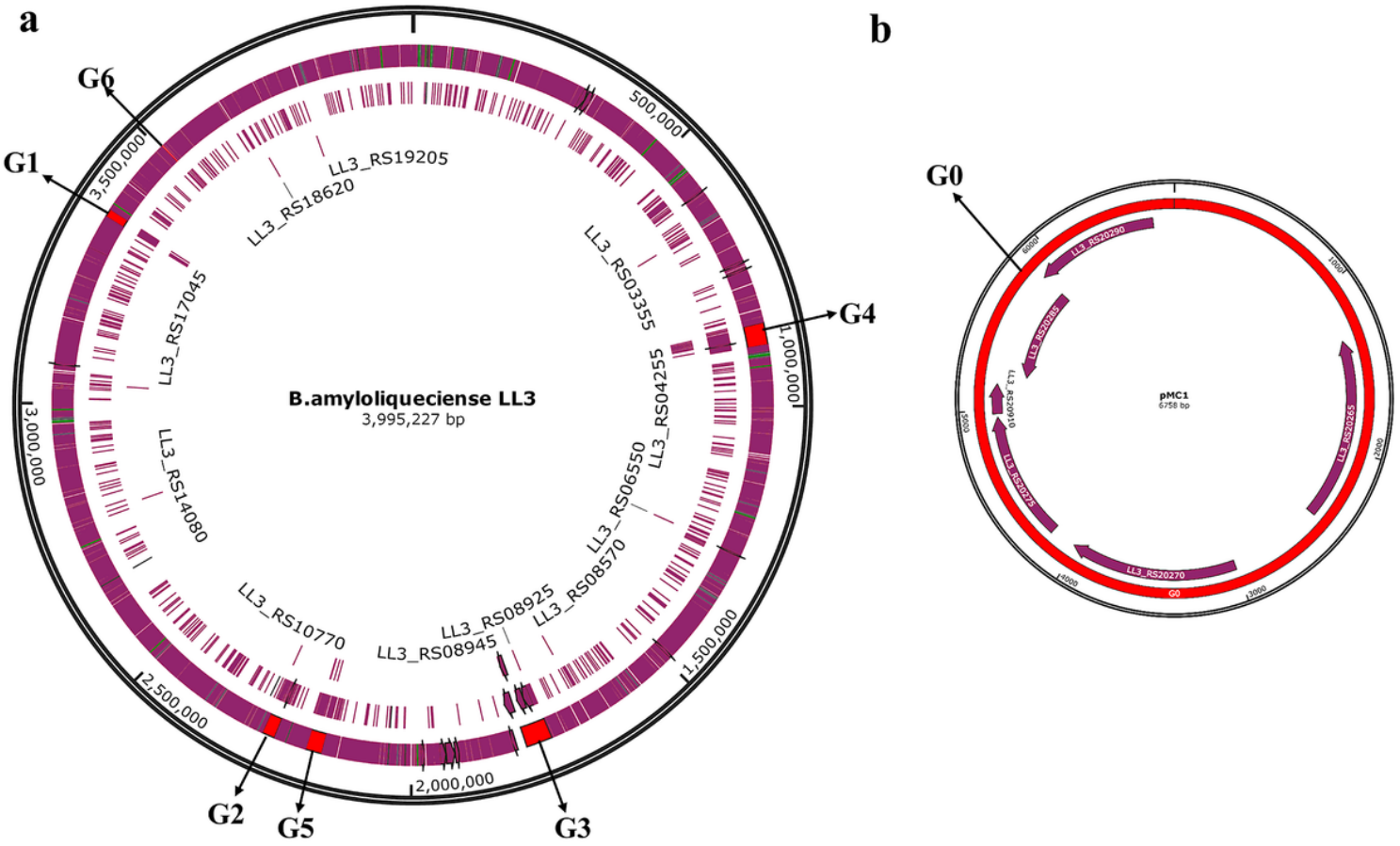

Figure 1

The construction of genome-reduced strain GR167. a The exact coordinates of the deleted regions (G1 to G6) on the chromosome of B. amyloliquefaciens LL3; b the physical map of the cured endogenous plasmid pMC1

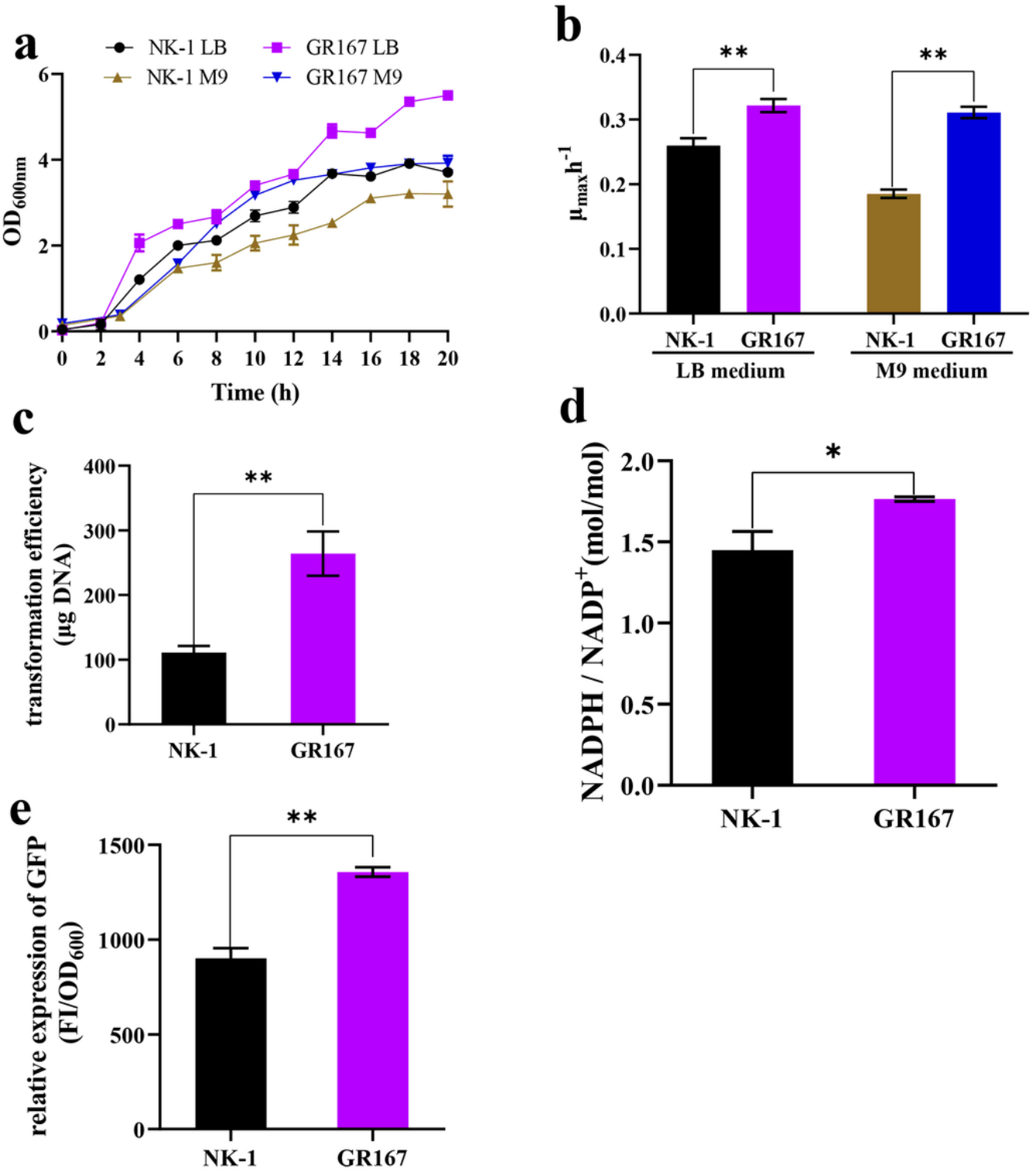

Figure 2

Physiological characteristics assessment of genome-reduced strain GR167 and the parental strain NK-1. a Growth curves; b maximum specific growth rate (μmax); c transformation efficiency; d intracellular reducing power level (NADPH/NADP+ molar ratio); e heterologous protein productivity (GFP, green fluorescent protein; FI, fluorescence intensity). Values denote mean ± SD of triplicates (*P < 0.05, **P < 0.01)

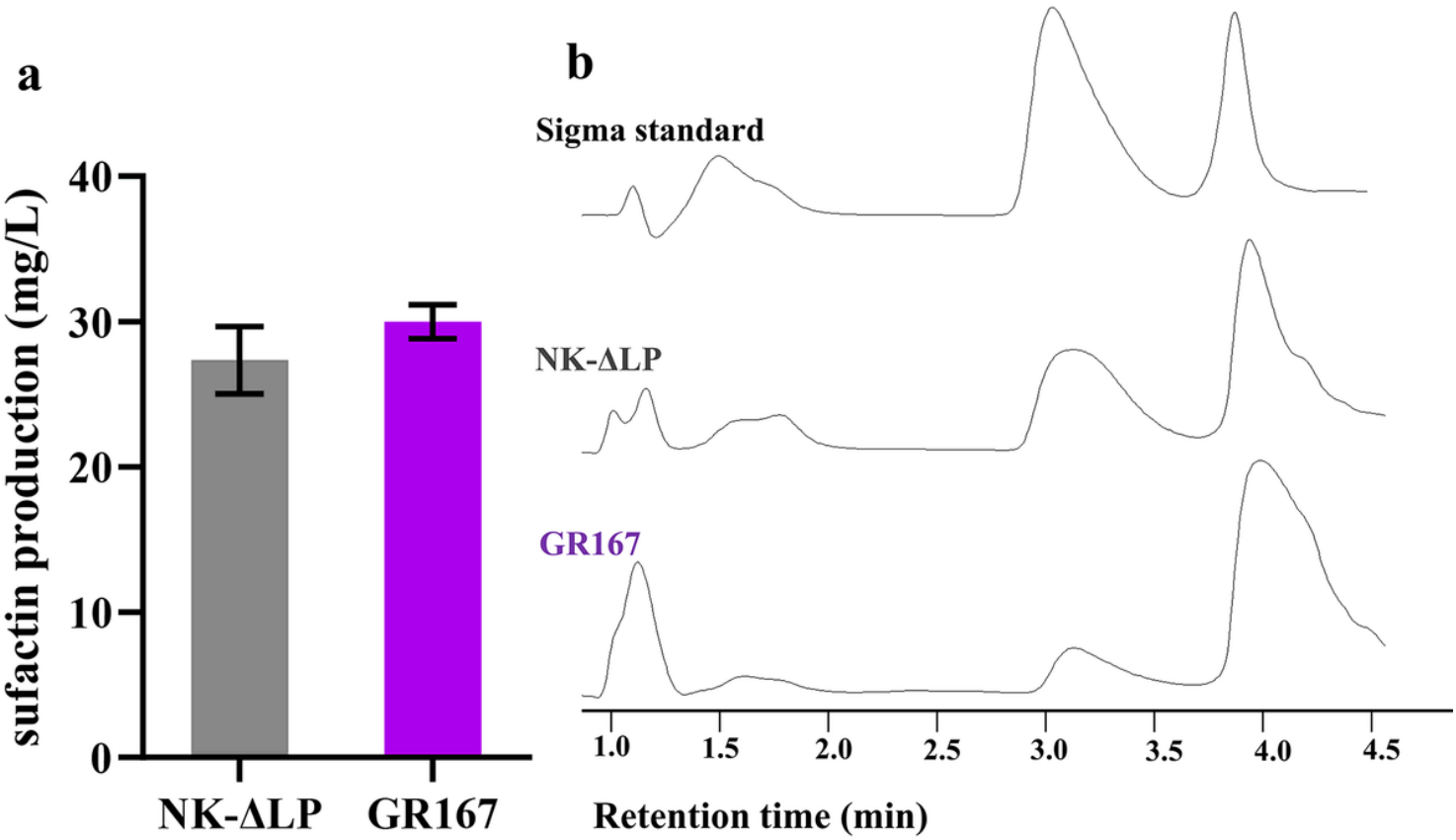

Figure 3

Surfactin biosynthesis by NK-ΔLP and genome-reduced strain GR167. a Surfactin production; b HPLC spectrograms of surfactin standard (Sigma) and produced surfactin samples. Values denote mean ± SD of triplicates

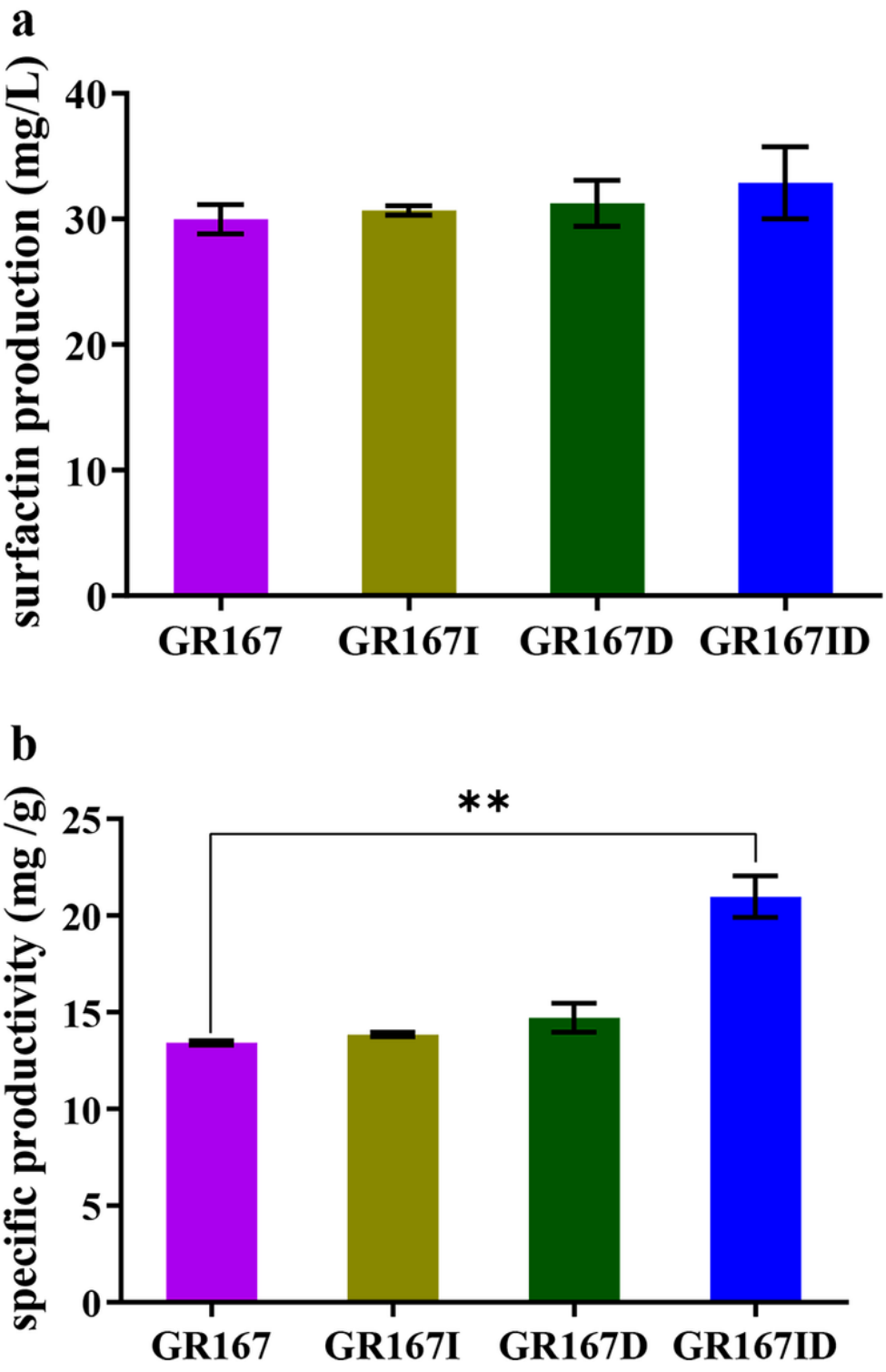

Figure 4

Surfactin production by GR167 and its derivatives (Δitu, Δfen). a Surfactin production; b specific productivity of surfactin (mg/g, the ratio of surfactin to CDW). To accumulate surfactin, the strains were incubated in Landy medium for 48 h at 30 °C and 180 rpm. Values denote mean ± SD of triplicates (**P < 0.01)

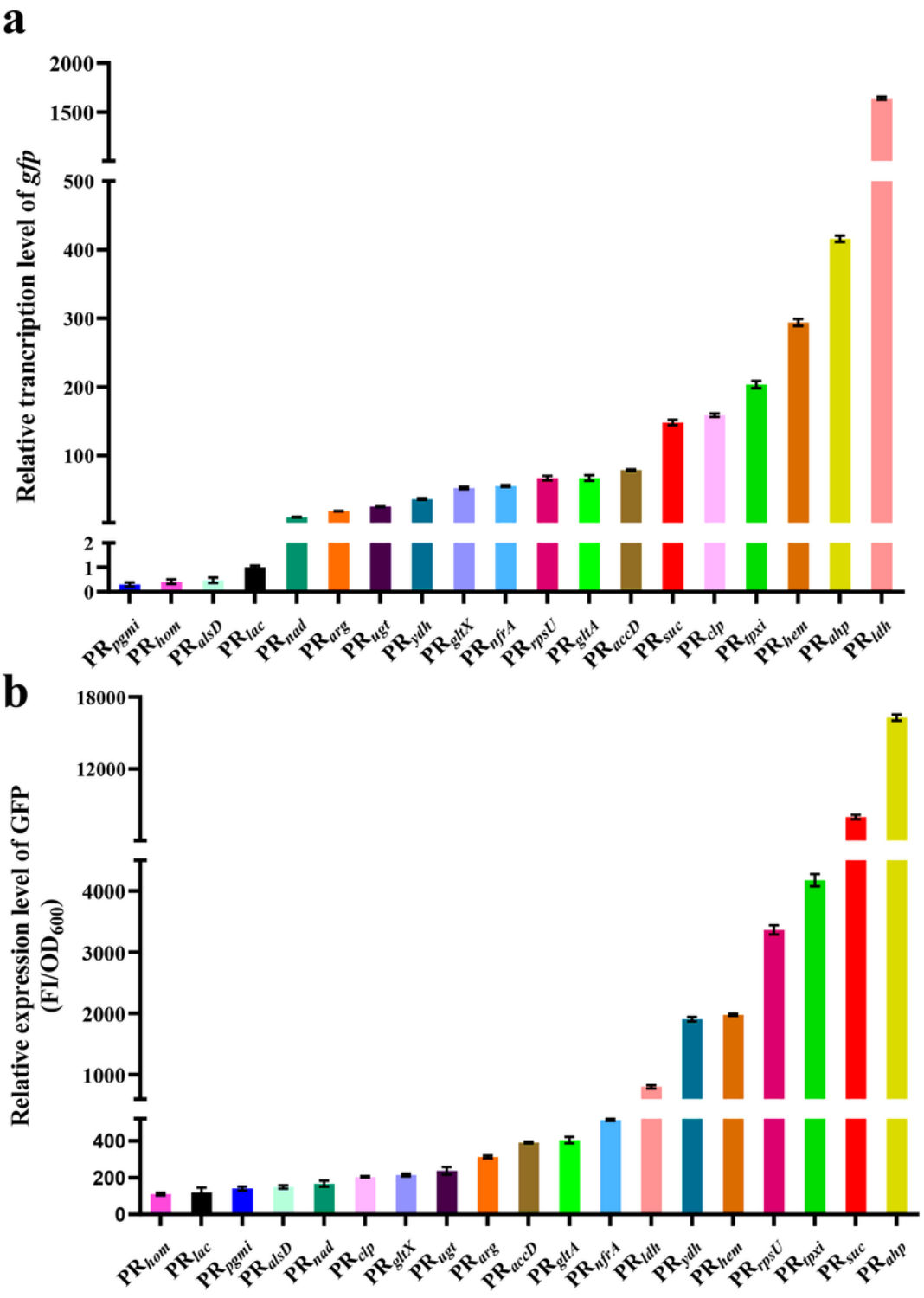

Figure 5

Characterization of the strengths of the selected endogenous promoters using reporter gene assays in LL3. a Transcriptional levels of gfp gene quantified via qPCR under the control of different promoters (rpsU gene was used as internal standard; the transcriptional level of gfp gene controlled by lac promoter was set as 1); b the relative fluorescence intensity of GFP (FI/OD600) under the control of different promoters. Values denote mean ± SD of triplicates

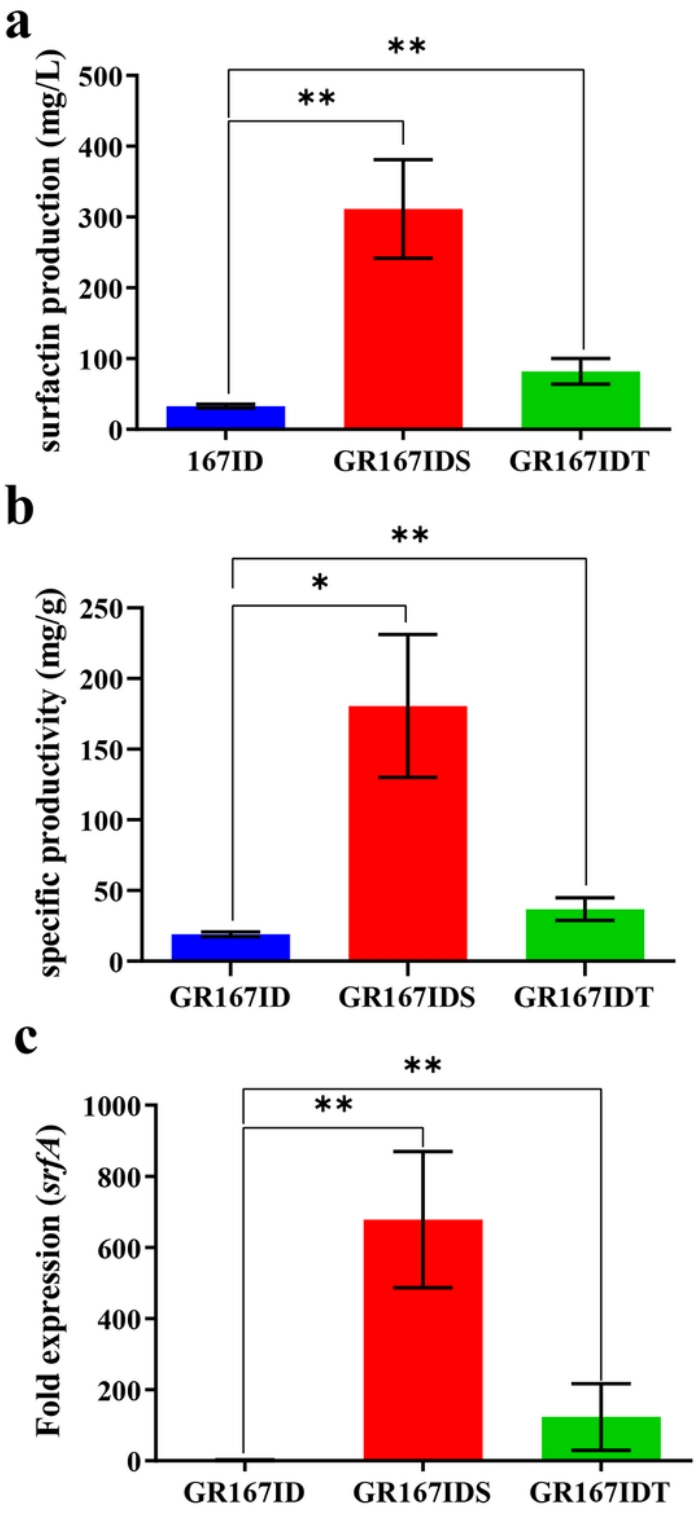

Figure 6

Surfactin production by GR167ID, GR167IDS and GR167IDT, and transcriptional levels of srfA operon in the strains. a Surfactin production; b specific productivity of surfactin (mg/g, the ratio of surfactin to CDW); c transcriptional levels of srfA operon quantified via qPCR (the transcriptional level of srfA operon in GR167ID was set as 1). Values denote mean ± SD of triplicates (*P < 0.05, **P < 0.01)

Supplementary Files

This is a list of supplementary files associated with this preprint. Click to download.

- SupplementaryMaterial.docx